Imaging Diagnosis of Various Hepatocellular Carcinoma Subtypes and Its Hypervascular Mimics: Differential Diagnosis Based on Conventional Interpretation and Artificial Intelligence

Yasunori Minami   Naoshi Nishida   Masatoshi Kudo

Department of Gastroenterology and Hepatology, Kindai University Faculty of Medicine, Osaka, Japan

Abstract
Background: Hepatocellular carcinoma (HCC) is unique among malignancies, and its characteristics on contrast imaging modalities allow for a highly accurate diagnosis. The radiological differentiation of focal liver lesions is playing an increasingly important role, and the Liver Imaging Reporting and Data System adopts a combination of major features including arterial phase hyper-enhancement (APHE) and the washout pattern. *Summary:* Specific HCCs such as well or poorly differentiated type, subtypes including fibrolamellar or sarcomatoid and combined hepatocellular-cholangiocarcinoma do not often demonstrate APHE and washout appearance. Meanwhile, hypervascular liver metastases and hypervascular intrahepatic cholangiocarcinoma can demonstrate APHE and washout. There are still other hypervascular malignant liver tumors (i.e., angiosarcoma, epithelioid hemangioendothelioma) and hypervascular benign liver lesions (i.e., adenoma, focal nodular hyperplasia, angiomyolipoma, flash filling hemangioma, reactive lymphoid hyperplasia, inflammatory lesion, arterioportal shunt), which need to be distinguished from HCC. When a patient has chronic liver disease, differential diagnosis of hypervascular liver lesions can be even more complicated. Meanwhile, artificial intelligence (AI) in medicine has been widely explored, and recent advancement in the field of deep learning has provided promising performance for the analysis of medical images, especially radiological imaging data contain diagnostic, prognostic, and predictive information which AI can extract. The AI research studies have demonstrated high accuracy (over 90% accuracy) for classifying lesions with typical imaging features from some hepatic lesions. The AI system has a potential to be implemented in clinical routine as decision support tools. However, for the differential diagnosis of many types of hypervascular liver lesions, further large-scale clinical validation is still required. *Key Messages:* Clinicians should be aware of the histopathological features, imaging characteristics, and differential diagnoses of hypervascular liver lesions to a precise diagnosis and more valuable treatment plan. We need to be familiar with such atypical cases to prevent a diagnostic delay, but AI-based tools also need to learn a large number of typical and atypical cases.

© 2022 The Author(s).
Published by S. Karger AG, Basel

Correspondence to:
Yasunori Minami, minkun@med.kindai.ac.jp

Introduction

Recent advances in imaging have contributed to significant improvements in early diagnosis and optimized patient management. Hepatocellular carcinoma (HCC) is unique among malignancies due to its characteristics on contrast imaging modalities, such as computed tomography (CT), magnetic resonance imaging (MRI), and ultrasonography, which allow for a highly accurate diagnosis [1–3]. Several guidelines for HCC have been developed by the use of imaging tests for diagnosis, and the American Association for the Study of Liver Diseases (AASLD) accepted the Liver Imaging Reporting and Data System (LI-RADS) criteria in 2018. The LI-RADS assigns a risk category for HCC to imaging observations in at-risk patients, and the CT/MRI LI-RADS adopts a combination of major features (size, nonrim arterial phase hyper-enhancement [APHE], nonperipheral washout, enhancing capsule, and threshold growth) [4]. In the USA, high specificity is required because patients with HCCs fundamentally receive treatment, including liver transplant, without biopsy for confirmation, and the LR-5 criteria could succeed to reach near 100% specificity for HCC [5]. APHE and the washout pattern have strong independent associations with HCC using LI-RADS [6]. Classic HCC is usually diagnosed by "arterial enhancement with delayed washout," and multiphase contrast-enhanced imaging is sufficiently accurate to diagnose HCC based on typical features on CT/MRI. However, there are many types of hypervascular liver lesions that need to be differentiated from typical HCC. Then, we sometimes encounter difficulties in seeing a delicate difference of tumor enhancement patterns between HCC and other hypervascular liver lesions.

Artificial intelligence (AI) in diagnosing diseases is a hot topic in the medical imaging and is an approach that analyzes data samples to make diagnoses using mathematical and statistical approaches, allowing machines to learn without programming. It is expected that a synergistic workflow that combines the experience of radiologists and the computational power of AI systems may substantially improve the efficiency and quality of clinical care. However, when the training datasets was not enough and the inputs were low in quality, even AI systems can be unreliable.

We need to be familiar with such atypical cases to prevent a diagnostic delay, but AI needs to learn a large number of typical and atypical cases as well. The main aim of this review was to present the typical and atypical imaging characteristics of HCC and other hypervascular liver lesions. Furthermore, the motivation behinds our review was to cover the basic principles of AI systems in diagnostic medical imaging and of their limitations.

Dynamics of Contrast Enhancement

Precontrast, arterial phase, portal venous phase, and delayed phase are all obtained for CT/MRI with extracellular agents. For MRI with hepatobiliary agents, a delay of 15–20 min for gadoxetic acid and a delay of 1 h for gadobenate dimeglumine consistently provide high-quality hepatobiliary phase (HBP) imaging. Delayed phase is acquired with extracellular agents or gadobenate after the portal venous phase [6]. Transitional phase is acquired with gadoxetic acid after the extracellular phase, before the HBP, but typically not obtained with gadobenate dimeglumine [6]. APHE is defined as enhancement in the arterial phase that unequivocally is greater than that of the surrounding liver [7]. Washout appearance is defined as a visually assessed temporal reduction in enhancement relative to the surrounding liver during the portal venous or delayed phase [7]. The term "washout appearance" is used as a typical feature of HCC.

LI-RADS attempts to standardize the interpretation of potentially complex CT and MRI findings for the diagnosis of HCC. Although CT and MRI produce images in different ways, contrast media for CT and MRI enters the liver through the hepatic artery and portal vein and is freely redistributed into the interstitial space [7, 8]. The pharmacokinetics of gadolinium chelates as MRI contrast agents mimic that of iodinated contrast agents for CT. Multiphasic CT, extracellular contrast-enhanced MRI, or gadolinium ethoxybenzyl diethylenetriamine penta-acetic acid (Gd-EOB-DTPA)-enhanced MRI is preferred for the diagnosis of HCC [1]. However, the amount of gadoxetate disodium in Gd-EOB-DTPA is only approximately 40% that of a conventional Gd-based agent. Therefore, vascular enhancement may be weakened on Gd-EOB-DTPA-enhanced MRI. Moreover, APHE can be missed if the arterial-dominant phase images are acquired too early.

Corona enhancement is observed as a rim of enhancement around hypervascular HCC in the late arterial phase and appears to reflect direct drainage into the surrounding liver tissue [9, 10]. During hepatocarcinogenesis, intratumor blood drains into the surrounding liver parenchyma through preserved portal veins within the capsule; therefore, HCC often shows thick corona

enhancement (>2 mm). The frequency of thick corona enhancement was 84.3% in hypervascular HCC and 11% in focal nodular hyperplasia (FNH) [11]. Thick corona enhancement is one of the imaging features of hypervascular HCC; however, corona enhancement is not specific to HCC because thin corona-like enhancement may be present in hypervascular metastases. Therefore, corona enhancement is included in the LI-RADS ancillary features for favoring malignancy in general, not HCC in particular [12].

Meanwhile, enhancing capsule is one of the major diagnostic features in the CT/MRI LI-RADS. Capsule appearance is observed as a rim of enhancement around hypervascular HCC in the delayed phase, owing to contrast material retention within fibrous capsule. However, Gd-EOB-DTPA starts to accumulate in normally functioning hepatocytes after administration. The detection of capsule enhancement can be limited due to hepatic parenchymal enhancement on MRI [13, 14]. Sensitivity and accuracy for the histologic capsule in the delayed phase on CT was highest among any phases of contrast enhanced CT or Gd-EOB-DTPA enhanced MRI. Thus, the capsule appearance can be noticed in the delayed phase on CT with high diagnostic performance.

HCC

HCC generally occurs in patients with cirrhosis or chronic liver disease. Approximately 80% of patients with newly diagnosed HCC have preexisting cirrhosis or chronic liver disease. However, HCC may develop in non-cirrhotic livers and shows similar patterns of enhancement to the more common HCC that occurs in cirrhotic livers.

Alterations in the hemodynamics of tumors occur during multistep hepatocarcinogenesis from a low-grade dysplastic nodule to moderately differentiated HCC. Arterial blood supply in nodules increases during hepatocarcinogenesis. Vascular collapse due to tumor growth may induce intertumoral hypoxia. In some cases of poorly differentiated HCC (p-HCC), tumor cells acquire a metabolic profile of increased glycolysis, which enables them to proliferate more rapidly under hypoxic conditions [15]. As a result, the arterial blood supply decreases when moderately differentiated HCC progresses to p-HCC. Therefore, most cases of early HCC and p-HCC include hypo-enhancing areas in the arterial phase (Table 1 and Fig. 1). Furthermore, p-HCC shows a shorter washout time than that of moderately differentiated HCC [16].

The enhancement pattern in the HBP on Gd-EOB-DTPA enhanced MRI has been explained by the expression of organic anion-transporting polypeptides and/or multidrug resistance-associated proteins (MRPs). Most cases of HCC are hypo-intense in the HBP because of the low expression of OATP1B3 and high expression of MRP2. However, 5–10% of HCC are iso- or hyper-intense relative to the liver in the HBP when MRP2 transporters excreting Gd-EOB-DTPA into the bile canaliculus decreased (Fig. 2) [17].

According to the 2019 WHO classification, eight subtypes defined by molecular characteristics such as steatohepatitic, clear cell, macrotrabecular-massive, scirrhous, chromophobe, fibrolamellar, neutrophil-rich, and lymphocyte-rich HCCs were identified [18]. Due to their unique cellular features, these subtypes may not demonstrate APHE and washout appearance, creating challenges in imaging diagnosis of HCC [19, 20]. By contrast, sarcomatoid HCC is now classified under the category of undifferentiated primary liver cancer. Sarcomatoid HCC is defined by extremely poor prognosis with a high risk of recurrence and metastasis. The imaging diagnosis of sarcomatoid HCC is also challenging because of its atypical image patterns such as hypodense or heterogeneous enhancement with a ring enhancing in the arterial phase and prolonged peripheral enhancement in the delayed phase [21, 22]. In addition, combined hepatocellular-cholangiocarcinoma (cHCC-CC) is also a rare hepatic malignancy that accounts for <1% of primary liver cancers [23]. cHCC-CC has heterogeneous imaging features because it is a tumor in which both HCC and ICC components coexist with various ratios and patterns. A diagnosis of cHCC-CC based on mixed patterns on images (progressive enhancement, arterial enhancement with washout, and an atypical pattern of arterial enhancement without washout and/or hypovascular lesions) was previously shown to have a sensitivity of 48% and specificity of 81% [24].

Other Hypervascular Liver Lesions

Multiphasic CT or dynamic contrast-enhanced MRI is recommended to be used first because of their higher sensitivity and the analysis of the whole liver by the international guidelines on the management of HCC [1–4]. Contrast-enhanced ultrasound is a second- or third-line diagnosis when CT and MRI are contraindicated or inconclusive [1–3].

Hypervascular Liver Metastases

Hypervascular metastases typically arise from primary neuroendocrine tumors, renal cell carcinoma, thyroid carcinoma, choriocarcinoma, or melanoma, and the enhance-

Table 1. Enhancement patterns of HCC and its hypervascular mimics

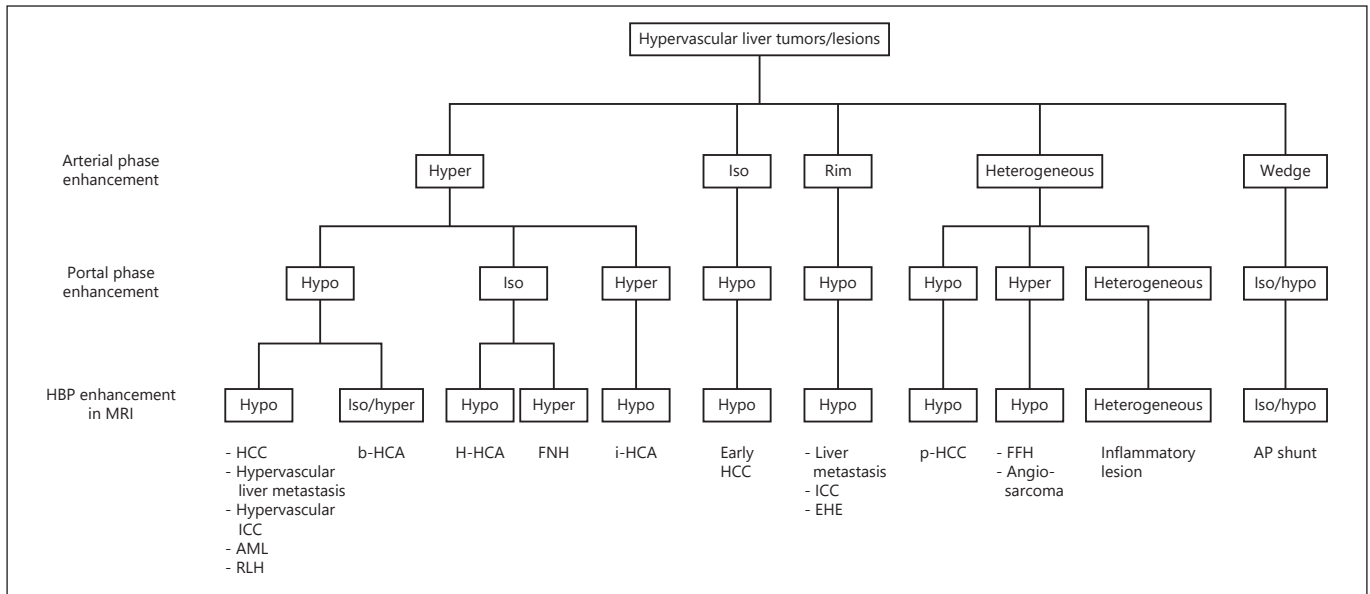| Tumor and subclass	Arterial phase	Portal venous phase	HBP in MRI
HCC			
Typical HCC	Hyper-enhancement	Hypo-enhancement (washout)	Hypo-intensity
Early HCC	Hypo- or iso-enhancement	Hypo-enhancement	Hypo-intensity
p-HCC	Heterogeneous hyper-enhancement	Hypo-enhancement	Hypo-intensity
Hypervascular liver metastases	Hyper-enhancement	Hypo-enhancement	Hypo-intensity
Hypervascular ICC	Hyper-enhancement	Hypo-enhancement	Hypo-intensity
HCA			
H-HCA	Hyper-enhancement	Iso-enhancement	Hypo-intensity
i-HCA	Hyper-enhancement	Persistent enhancement	Hypo-intensity
β-catenin-activated type	Hyper-enhancement	Hypo-enhancement	Iso- or hyper-intensity
FNH	Hyper-enhancement	Iso- or slightly hyper-enhancement	Hyper-intensity
AML	Hyper-enhancement	Hypo-enhancement	Hypo-intensity
Primary hepatic malignant vascular tumors			
Angiosarcoma	Heterogeneous hyper-enhancement	Centripetal enhancement	Hypo-intensity
Epithelioid hemangioendothelioma	Rim enhancement	Hypo-enhancement	Hypo-intensity
FFH	Heterogeneous hyper-enhancement	- Hyper-enhancement with extracellular contrast agents - Iso- or hypo-enhancement with gadoxetate	Hypo-intensity
Reactive lymphoid hyperplasia	Hyper-enhancement	Hypo-enhancement	Hypo-intensity
Inflammatory lesion	Rim or heterogeneous enhancement	Heterogeneous enhancement with hypodense areas	Heterogeneous hypo-intensity
AP shunt	Wedge or cone-shaped hyper-enhancement	Iso- or hypo-enhancement	Iso- or slightly hypo-intensity

HNF1α, hepatocyte nuclear factor 1α.

Fig. 1 flowchart:

Hypervascular liver tumors/lesions

Arterial phase enhancement	Portal phase enhancement	HBP enhancement in MRI	Diagnosis
Hyper	Hypo	Hypo	- HCC - Hypervascular liver metastasis - Hypervascular ICC - AML - RLH
Hyper	Hypo	Iso/hyper	b-HCA
Hyper	Iso	Hypo	H-HCA
Hyper	Iso	Hyper	FNH
Hyper	Hyper	Hypo	i-HCA
Iso	Hypo	Hypo	Early HCC
Rim	Hypo	Hypo	- Liver metastasis - ICC - EHE
Heterogeneous	Hypo	Hypo	p-HCC
Heterogeneous	Hyper	Hypo	- FFH - Angiosarcoma
Heterogeneous	Heterogeneous	Heterogeneous	Inflammatory lesion
Wedge	Iso/hypo	Iso/hypo	AP shunt

Fig. 1. Diagnostic flowchart for HCC and its hypervascular mimics. The procedure is based on the intensity and heterogeneity of enhancement in the arterial and portal phases on CT/MRI and HBP on MRI. AML, angiomyolipoma; AP shunt, arterioportal shunt; EHE, epithelioid hemangioendothelioma; FFH, flash filling hemangioma; FNH, focal nodular hyperplasia; HBP, hepatobiliary phase; HCA, hepatocellular adenoma; b-HCA, β-catenin-activated HCA; H-HCA, HNF-1α-inactivated HCA; i-HCA, inflammatory HCA; HCC, hepatocellular carcinoma; p-HCC, poorly differentiated HCC; ICC, intrahepatic cholangiocarcinoma.

ment pattern such as APHE with washout is similar to or indistinguishable from that of classic HCC (Table 1 and Fig. 1). Liver metastases from colon, lung, breast, or gastric carcinomas generally show enhancement at the peripheral or perilesional regions in the arterial phase and washout in the portal venous and/or delayed phase. However, homogeneous arterial hypervascularity can be depicted in breast adenocarcinoma liver metastases though in rare cases [25].

Hypervascular Intrahepatic Cholangiocarcinoma

The predominant radiological image of intrahepatic cholangiocarcinoma (ICC) is a hypovascular mass with peripheral enhancement and gradual centripetal contrast enhancement on dynamic studies because its main pathological feature is adenocarcinoma with a fibrotic and hypovascular stroma [8]. However, small ICC (≤3 cm in diameter) may show atypical enhancement patterns (arterial enhancement and/or washout in the portal venous phase) typically of a small-duct origin [18] (Fig. 3). This enhancing behavior can be interpreted by less intratumoral fibrosis and abundant vascular stroma. An important consideration is the finding of hypervascularity and arterial phase enhancement on images in approximately 10% of ICC cases [26]. Since hypervascular ICCs are often seen in cirrhotic livers, the differential diagnosis with HCC can be difficult. However, the combination of APHE and washout appearance is rarely observed in ICC [27] (Table 1 and Fig. 1).

Hepatocellular Adenoma

Hepatocellular adenoma (HCA) is a benign tumor that essentially develops in young women taking oral contraceptives. The incidence of HCA is approximately 1–3 million cases per year in Europe and North America but is lower in Asia. Four subtypes of HCA are recognized: hepatocyte nuclear factor 1α (HNF-1α)-inactivated type, β-catenin-activated type, inflammatory type, and unclassified type [28, 29]. Additionally, HCAs with β-catenin mutations frequently undergo malignant change and inflammatory HCAs (i-HCA) commonly bleed. HNF-1α-inactivated HCAs (H-HCAs) approximately count for 35–40% of all HCAs. In patients with germline H-HCAs, familial HCA occurred equally in male and female [30]. These demonstrate hyper-enhancement in the arterial phase and iso-enhancement in the portal venous and delayed phases. i-HCAs count for 30–35% of all HCAs. These usually show arterial hyper-enhancement and persistent enhancement in the portal venous and delayed phases. i-HCAs may show heterogeneity or ring enhancement in the HBP images. β-Catenin activated HCAs count for 20% of all HCAs, occur
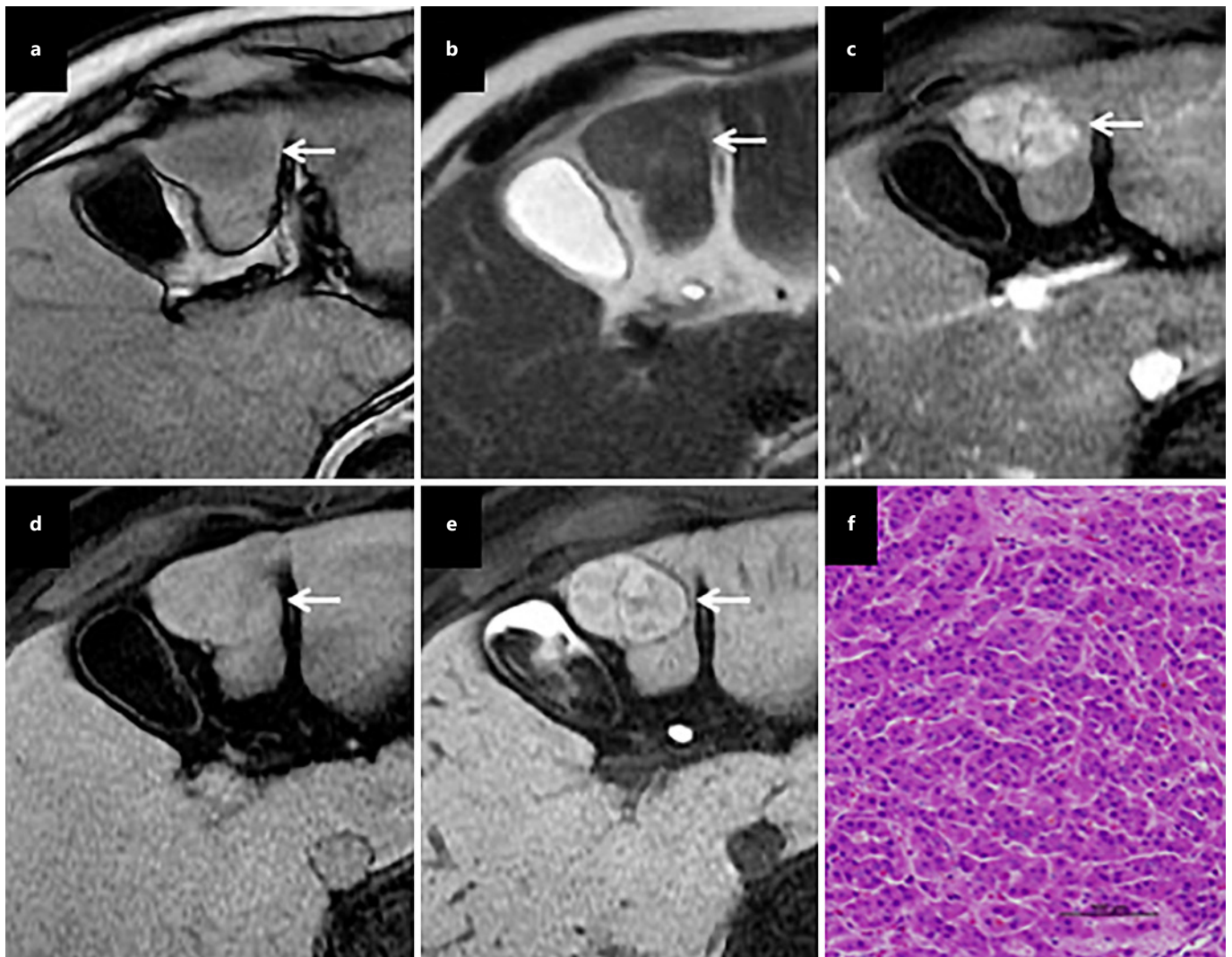
Fig. 2. High signal intensity of HCC in the HBP. A tumor (arrow) presents with low intensity on T1WI (**a**), slight hyper-intensity on T2WI (**b**), hyper-enhancement in the arterial phase (**c**), iso-intensity in the portal phase (**d**), and hyper-intensity in the HBP (**e**). A pathological diagnosis of moderately differentiated HCC was established (**f**).

more frequently in men (up to 38% of lesions are found in males), and are only rarely multiple [31]. These can demonstrate strong arterial enhancement with portal venous washout. Especially, pooled proportion of iso- or hyper-intensity in the HBP on MRI was 14% among all HCAs, 0% among H-HCAs, 11% among unclassified HCAs, 14% among i-HCAs, and 59% among β-catenin-activated HCAs [29].

FNH/FNH-Like Lesion

FNH is not a true neoplasm. It is a benign hepatic lesion with a central scar and radiating fibrous cords. It may be caused by a regenerative response to local vascular

anomalies and is seen in patients without chronic liver disease. The strong homogeneous enhancement of well-delineated, lobular-shaped FNH is observed in the arterial phase with a hypodense central scar on dynamic contrast-enhanced CT and MRI [8]. FNH appears isodense in the portal venous and delayed phases on dynamic contrast-enhanced CT. The central scar and septations typically show late enhancement due to the diffusion of contrast material into the stroma of the lesion. On dynamic contrast MRI, the lesion is slightly hyper-intense with a hypo-intense central scar in the portal venous phase [8]. In addition, FNH is typically hyper- or iso-intense in the HBP on
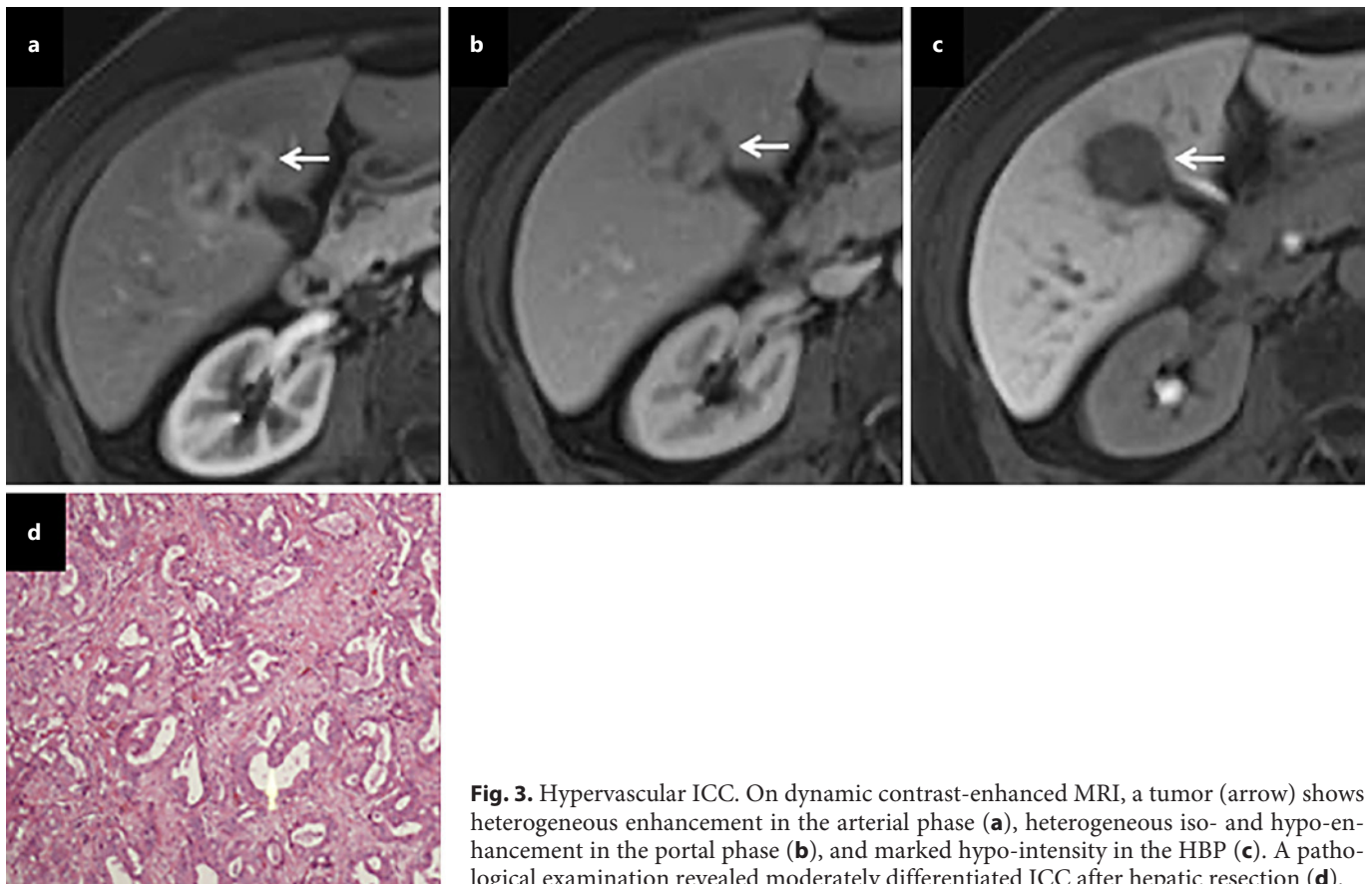
Fig. 3. Hypervascular ICC. On dynamic contrast-enhanced MRI, a tumor (arrow) shows heterogeneous enhancement in the arterial phase (**a**), heterogeneous iso- and hypo-enhancement in the portal phase (**b**), and marked hypo-intensity in the HBP (**c**). A pathological examination revealed moderately differentiated ICC after hepatic resection (**d**).

Gd-EOB-DTPA-enhanced MRI because it comprises functioning hepatocytes and bile ducts. Overall, 96.9% of FNH are either iso- or hyper-intense relative to the liver parenchyma, while 3.1% are hypo-intense in the HBP [32]. Moreover, HBP enhancement was homogeneous in 68% of FNH lesions, heterogeneous in 18%, and peripheral in 14% [32] as FNH can have various patterns of imaging features.

FNH-like lesions often occur in patients with alcoholic liver cirrhosis or liver vessel abnormalities. FNH-like lesions are multiple, and they can show APHE and hypo-intensity in the HBP [8]. Then, a case of FNH-like nodule in liver cirrhosis might be misdiagnosed as HCC. Some of these nodules are considered as the same entity as i-HCA [33].

Angiomyolipoma

Angiomyolipoma (AML) is a mesenchymal tumor made up of abnormal blood vessels, spindle cells, and mature adipocytes, believed to be derived from perivascular epithelioid cells (PECs), and PEComa is a family of mesenchymal tumors arising from PECs including AML. Hepatic AML is a relatively rare benign mesenchymal tumor that comprises the three histological components of blood vessels, smooth muscle, and adipose tissue. The main characteristics of AML are the presence of both fat and prominent vascularity in tumor lesions. On plain CT, AML presents as a well-defined solid heterogeneous mass containing a markedly hypodense area due to the fatty component. This fatty component shows hyper-intensity on both T1- and T2-weighted MRI, which is suppressed by various fat suppression techniques. In cases with fat-poor AML, chemical shift imaging (i.e., in-phase/out-of-phase) is useful for detecting a small fat content. Marked enhancement in the arterial phase may be observed on dynamic CT and/or MRI because of the vascular component (Table 1 and Fig. 1) (Fig. 4). Although the frequency of washout on portal phase images was previously shown to be lower for AML than for HCC, 61.1% of AML were still hypo-intense in the portal phase [34].

Variations have been reported in the imaging characteristics of hepatic AML that appear to be dependent on the proportions of its different components. Difficulties
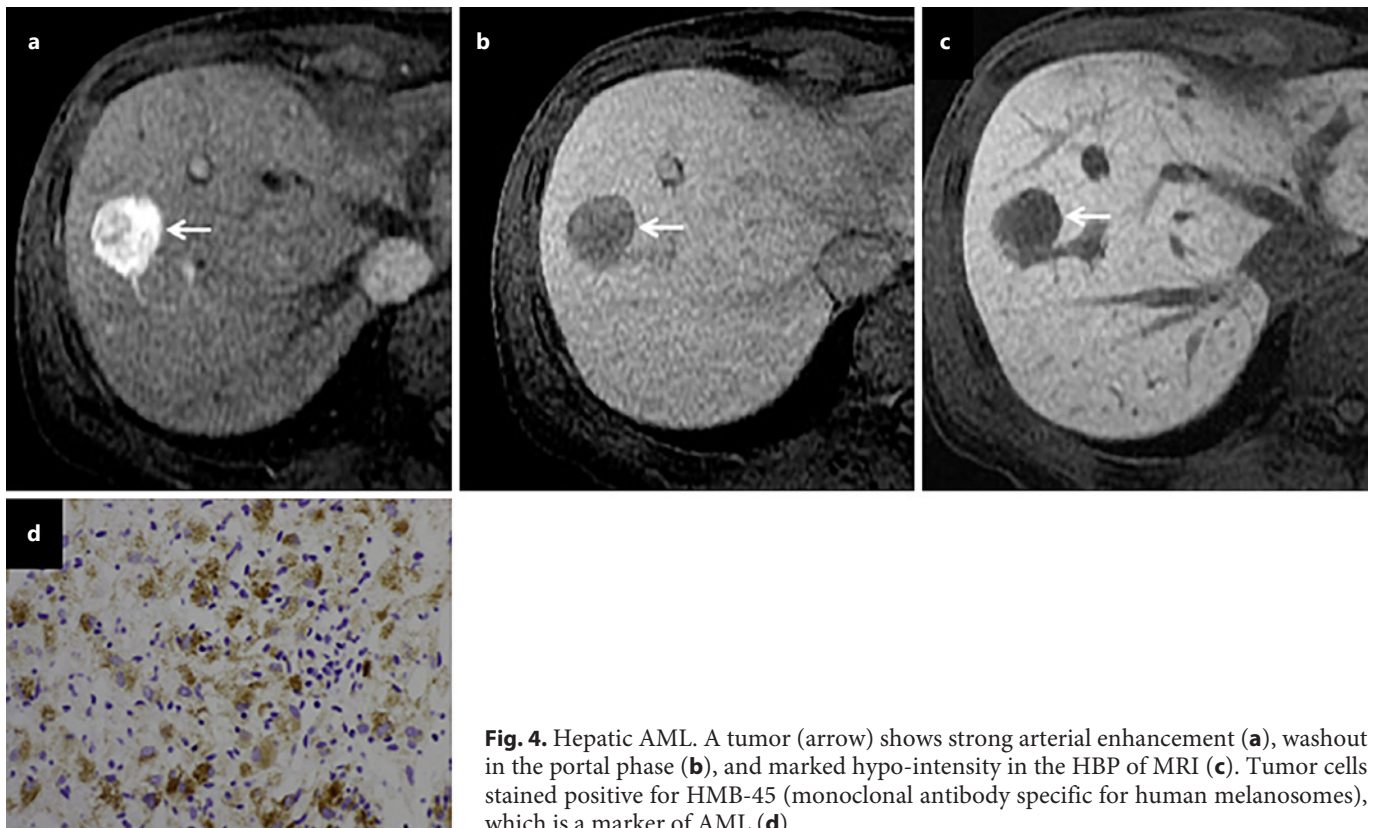
Fig. 4. Hepatic AML. A tumor (arrow) shows strong arterial enhancement (**a**), washout in the portal phase (**b**), and marked hypo-intensity in the HBP of MRI (**c**). Tumor cells stained positive for HMB-45 (monoclonal antibody specific for human melanosomes), which is a marker of AML (**d**).

are still associated with accurately diagnosing AML; however, drainage via the hepatic veins may be a key feature for differentiating it from fat-containing HCC that mainly drains into the portal vein. Dynamic CT may achieve detection frequencies of 80–83.3% for early draining veins in patients with AML [35].

Primary Hepatic Malignant Vascular Tumors

Primary hepatic malignant vascular tumors are a rare type of tumor that comprises different vascular components and may be characterized by its malignant potential (epithelioid hemangioendothelioma, PEC tumor, and solitary fibrous tumor) and malignancy (angiosarcoma) [35]. On CT and MRI, most primary hepatic malignant vascular tumors are ill-defined, heterogeneous, hypervascular masses with centripetal progressive enhancement and possibly calcification. Solid components are significantly enhanced in the arterial phase (Table 1). Epithelioid hemangioendothelioma and solitary fibrous tumors, including hemangiopericytoma, may present with arterial enhancing rim and hypo-enhancement in the portal venous phase, while hepatic angiosarcoma shows rim or irregular nodular enhancement in the arterial phase and

centripetal enhancement in the portal venous phase (Fig. 5) [36, 37]. In the HBP of Gd-EOB-DTPA-enhanced MRI, primary hepatic malignant vascular tumors have predominantly low signal intensity [36, 37].

Flash Filling Hemangioma

The majority of hepatic hemangioma typically shows peripheral nodular enhancement with gradual central fill-in and sustained enhancement [8]. However, flash filling hemangioma (FFH) is a subtype of hepatic hemangioma and is also known as high flow hemangioma or capillary hemangioma. This subtype composes of 16% of all hepatic hemangiomas. FFH is generally smaller in size (<2 cm) and often shows complete homogeneous enhancement in the arterial phase without a central fill-in pattern on CT and MRI (Table 1 and Fig. 1). The washout of FFH (lower attenuation than in the parenchyma) is not common. However, approximately 50% of FFH shows iso-enhancement in the transitional or delayed phase (Fig. 6) [38].

Reactive Lymphoid Hyperplasia or Pseudolymphoma

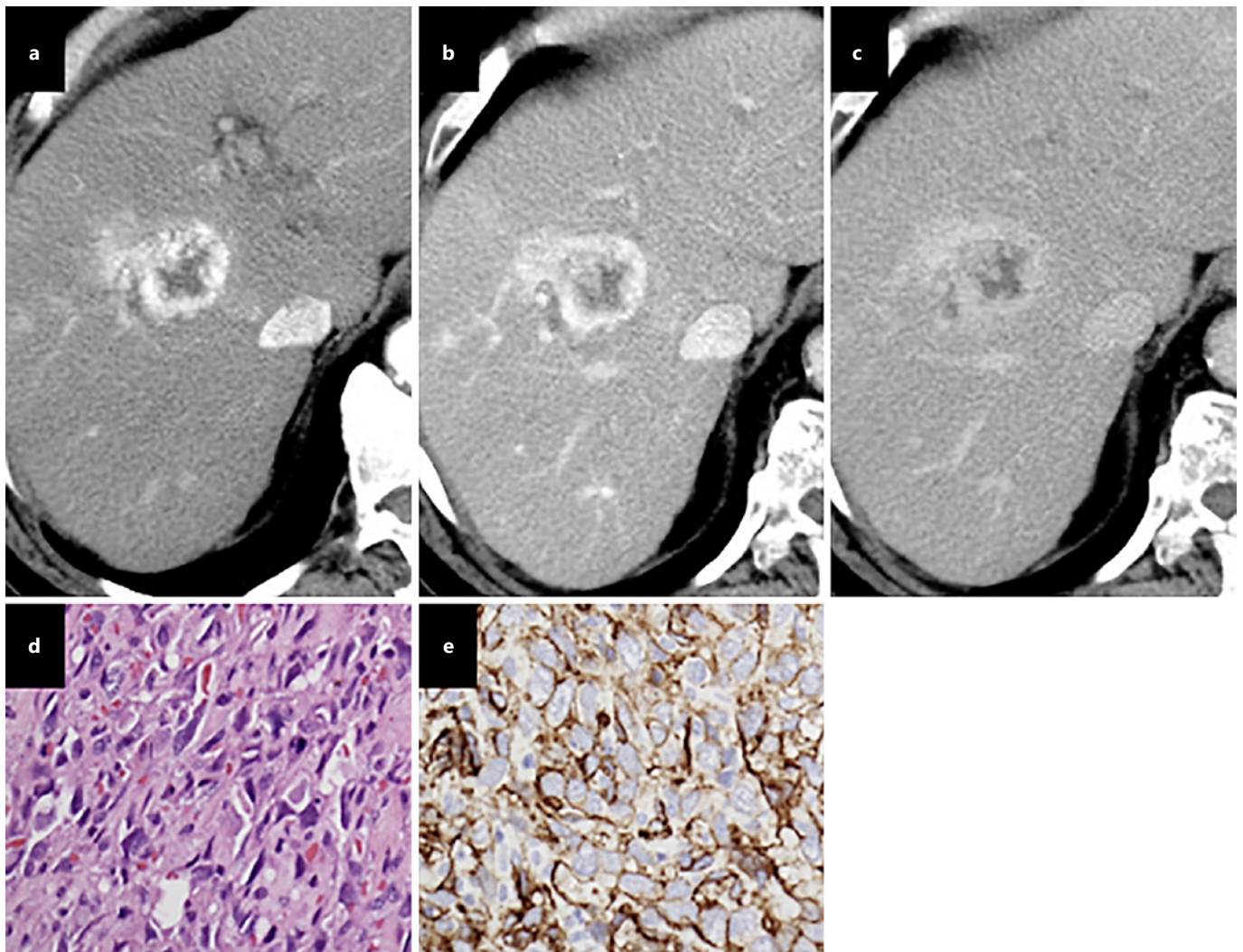Reactive lymphoid hyperplasia of the liver, also known as hepatic pseudolymphoma, is a rare hepatic

Fig. 5. Hepatic angiosarcoma. On contrast administration, early arterial peripheral vascularity in segment V (**a**), a tumor was seen with centripetal enhancement in the portal (**b**) and equilibrium phases (**c**). The tumor cells are spindle-shaped, with ill-defined borders, a slightly eosinophilic cytoplasm, hyperchromatic elongated nuclei; mitotic figures are frequently seen on a hematoxylin eosin staining image (**d**), and CD34 immunostaining highlights the tumor cells along with blood vessels (**e**).

nodular lesion that forms a liver mass that typically shows polyclonal lymphocytic cell proliferation without prominent nuclear atypia, with the formation of follicles and germinal centers. The prognosis of hepatic reactive lymphoid hyperplasia is favorable because of the low risk of recurrence or progression to lymphoma. A low-density lesion on plain CT, mild to moderate enhancement in the arterial phase, and hypodense areas in the portal phase may be observed (Table 1 and Fig. 1). MRI generally shows hypo-intensity on T1-weighted images, hyper-intensity on T2-weighted images, hypervascularity in the arterial phase, hypodense

areas in the portal phase, and is unclear in the delayed phase [39]. Furthermore, hyper-intensity on diffusion-weighted imaging and hypo-intensity in the HBP have been reported [40].

Inflammatory Lesion

Inflammatory lesions of the liver include liver abscess, inflammatory pseudotumor, and granulomatous inflammation. Although imaging features vary according to the inflammatory stage, multiphasic CT depicted peripheral/rim enhancement during the arterial phase in 82.5% and heterogeneous contrast enhancement with hypodense ar-
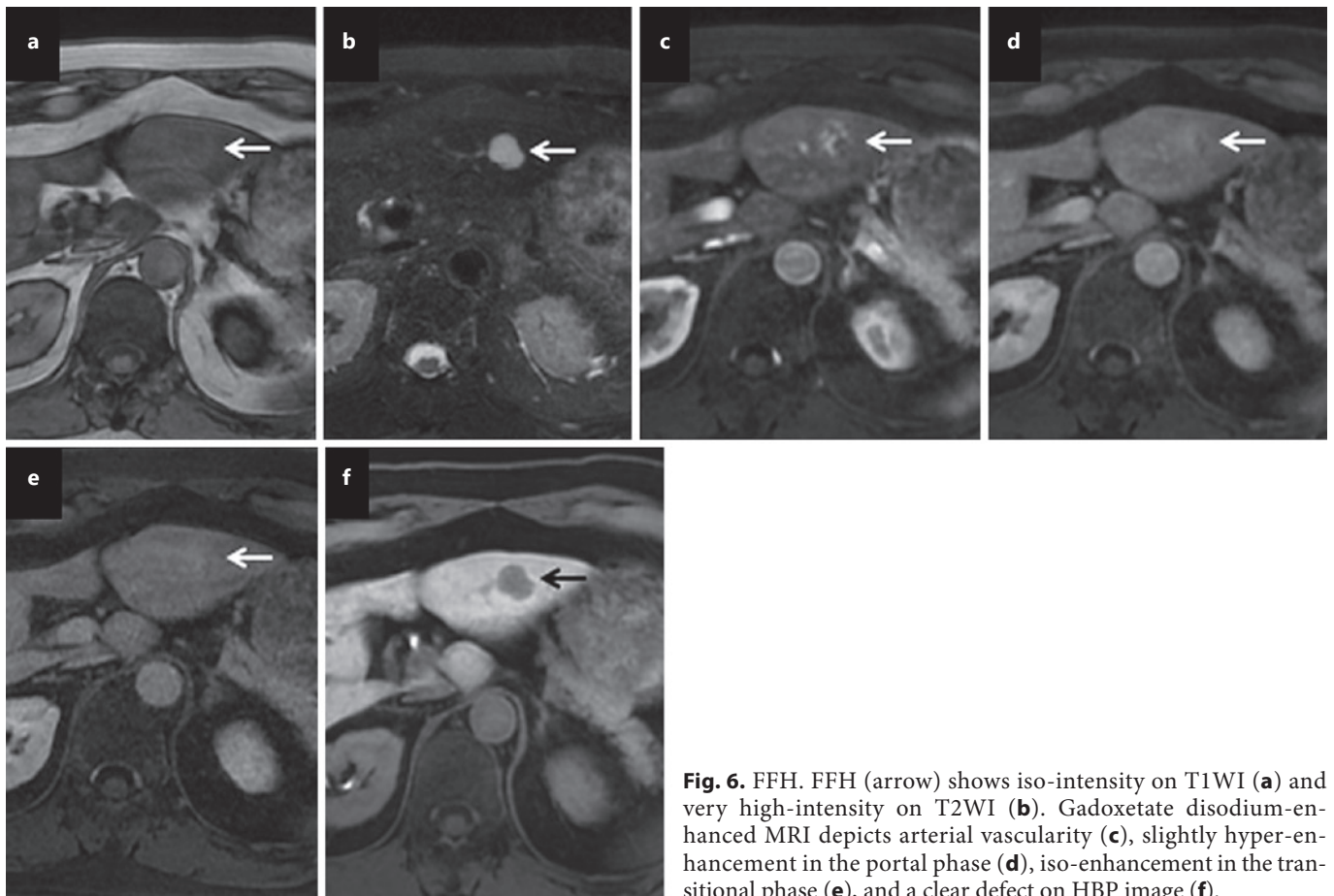
Fig. 6. FFH. FFH (arrow) shows iso-intensity on T1WI (**a**) and very high-intensity on T2WI (**b**). Gadoxetate disodium-enhanced MRI depicts arterial vascularity (**c**), slightly hyper-enhancement in the portal phase (**d**), iso-enhancement in the transitional phase (**e**), and a clear defect on HBP image (**f**).

eas during the delayed phase in 77.0% [41]. Gd-EOB-DT-PA-enhanced MRI showed peripheral rim-like enhancement in 77.8% [41]. In these cases, the major issue is to distinguish inflammatory lesions of the liver from atypical HCC, ICC, metastatic tumor.

Arterioportal Shunt

Hepatic arterioportal (AP) shunt is a type of hemodynamic abnormality such as a macroscopic AP fistula or transtumoral shunt. It sometimes demonstrates a peripheral, wedge, or cone-shaped hyper-enhancing area with a straight margin and/or contains normal vessels. In addition, imaging findings such as the gradual decrease of hyper-enhancement and no corona enhancement may be helpful for differential diagnosis. AP shunt usually shows iso-enhancement in the HBP on Gd-EOB-DTPA-enhanced MRI. However, it should be noted that AP shunt may show slightly hypo-enhancement in the HBP due to locally impaired hepatocytic function [8]. When AP shunt showed a round

shape, this may complicate the differential diagnosis. Moreover, considerable overlap between AP shunt and HCC is observed.

AI in Diagnostic Medical Imaging

Basics and Background

AI refers to the ability of a machine to simulate human intelligence [42]. Deep learning which is a sub-discipline of AI is designed using numerous layers of convolutional neural networks (CNNs). Each of neural networks provides a different interpretation of the data that has been fed to them, and deep learning can allow analysis of unstructured data and automated identification of features. Training data are the key input for learning, and having the right quality and quantity of data sets is very important to get accurate results. Insufficient data will impair a model prediction accuracy, while more than enough data can give the best results.

Supervised learning, unsupervised learning, and reinforcement learning are the three major paradigms for deep learning [42]. Supervised learning requires paired data samples for the inputs and the correct outputs. The algorithm measures its accuracy through the loss function, adjusting until the error has been sufficiently minimized. Unsupervised learning models work on their own to discover the inherent structure of unlabeled data. However, unsupervised learning models are computationally complex because they need a large training set to produce intended outcomes, and powerful tools are needed for working with large amounts of unclassified data. Reinforcement learning determines the optimal behavior in an environment to obtain maximum reward over time. Although no straightforward loss function is available in the reinforcement learning technique, the main drawback of reinforcement learning is that parameters may influence the speed of learning. Two categories of AI in liver imaging are radiomics (relying on classical machine learning) and deep learning systems (relying on CNNs). They are considered supervised learning approaches because both approaches aim to predict a pre-defined ground truth.

Present and Future Perspectives

Potential applications of AI for diagnosis of focal liver lesions (FLLs) include lesion detection, lesion tracking over serial examinations, imaging feature characterization, and LI-RADS categorization. Das et al. [43] introduced a new methodology for the automatic detection of liver tumors in CT images. A total of 225 images were used in this work to develop the proposed model. After tumor segmentation, three types of FLLs such as HCC, liver metastasis, and hemangioma were automatically classified. Thus, 99.38% accuracy for classification could be achieved. From multiple sequences of Gd-EOB-DTPA-enhanced MRI, AI-based application achieved an area under the curve (AUC) of 0.98 for accurate differentiation of FLLs including HCC, liver metastasis, and FNH [44]. Moreover, a 92% accuracy, a 92% sensitivity, and a 98% specificity could be demonstrated for classifying lesions with typical imaging features from six FLLs including HCC, ICC, colorectal cancer metastasis, hemangioma, FNH, and simple cyst [45].

Yamashita R et al. [46] developed a CNN model for assigning LI-RADS categories to liver observations on multiphase CT and MRI using a relatively small dataset through transfer learning and data augmentation techniques. For model development, a dataset comprising axial multiphase contrast-enhanced images in the Joint Photograph Experts Group (JPEG) format was used,

and images were annotated with corresponding observation diameters. In total, the LR-Atlas dataset included 314 observations: LR-1/2 ($n = 89$), LR-3 ($n = 62$), LR-4 ($n = 65$), and LR-5 ($n = 98$). Two distinct models were developed using two CNN architectures, and the transfer learning model outperformed the custom-made model: overall accuracy of 60.4% and AUCs of 0.85, 0.90, 0.63, 0.82 for LR-1/2, LR-3, LR-4, LR-5, respectively. However, the transfer learning CNN had an inferior performance on external CT and MRI datasets than on the internal held-out test set because the inputs were not high in quality as a result. The transfer learning model interpreted geographic fat deposition, confluent fibrosis, hypertrophic pseudomass, nodule-like APHE, and distinctive LR-1/2 observations as malignant hepatic nodules. Recently, the systematic review report stated that radiomics or deep learning systems have high performances in liver nodules classification, sometimes similar or better than human evaluation [47]. The best performance of deep learning was an AUC of 0.95 on MRI, and the best performance of radiomics was AUC of 0.98 either on CT and MRI, while the lower ones were, respectively, AUC of 0.63 either on CT and MR for DL and AUC of 0.70 on CT for radiomics.

Although the results showed their potential reliability as a powerful tool that can improve clinicians' performances, AI-based tools have not yet reached full diagnostic potential. Despite the latest innovations in machine learning technology, AI systems still do not provide information about the factors used in decision-making in a manner that can be understood by radiologists and physicians, which prevents them from incorporating their results into an informed decision-making process [48–50]. AI systems showing high accuracy in a more transparent manner are more likely to gain clinical acceptance. However, the medical profession will never be replaced by AI in the future. We should not accept the predictions of AI models without questioning and be aware of the limitations for acceptance and utilization of AI-based tools as much as their abilities.

Conclusion

This review comprehensively describes atypical HCC enhancement patterns for different histological grades as well as the key points for an imaging diagnosis of a benign and malignant hypervascular liver tumor that needs to be differentiated from HCC. When a patient has chronic liv-

er disease, differential diagnosis of hypervascular liver lesions can be even more complicated. Therefore, familiarity with these mechanisms, causes, types, degrees, imaging features, and differential diagnoses of hypervascular liver lesions will allow the clinicians to make a precise diagnosis and provide the more valuable treatment plan for patients.

The use of AI is growing rapidly in the medical field, especially in diagnostics. The AI system has a potential to be implemented in clinical routine as decision support tools. However, for the diagnosis of various types of hypervascular liver lesions, this still requires further large-scale clinical validation.

Statement of Ethics

This manuscript is a review of published studies, and no new research activities involving human subjects were performed. Therefore, an institutional or ethical review was not considered necessary by the authors.

Conflict of Interest Statement

Funding Sources

Author Contributions

The manuscript was conceived and designed by Yasunori Minami, Naoshi Nishida, and Masatoshi Kudo. Data acquisition was performed by Yasunori Minami. Data were analyzed and interpreted by Yasunori Minami, Naoshi Nishida, and Masatoshi Kudo. The manuscript was drafted by Yasunori Minami. All the authors revised the manuscript for important intellectual content, and all the authors approved the final version of the manuscript.

References

1 Roberts LR, Sirlin CB, Zaiem F, Almasri J, Prokop LJ, Heimbach JK, et al. Imaging for the diagnosis of hepatocellular carcinoma: a systematic review and meta-analysis. Hepatology. 2018;67(1):401–21.

2 Chou R, Cuevas C, Fu R, Devine B, Wasson N, Ginsburg A, et al. Imaging techniques for the diagnosis of hepatocellular carcinoma: a systematic review and meta-analysis. Ann Intern Med. 2015 19;162(10):697–711.

3 Kudo M, Kawamura Y, Hasegawa K, Tateishi R, Kariyama K, Shiina S, et al. Management of hepatocellular carcinoma in Japan: JSH consensus statements and recommendations 2021 update. Liver Cancer. 2021;10(3):181–223.

4 Chernyak V, Fowler KJ, Kamaya A, Kielar AZ, Elsayes KM, Bashir MR, et al. Liver Imaging Reporting and Data System (LI-RADS) version 2018: imaging of hepatocellular carcinoma in at-risk patients. Radiology. 2018; 289(3):816–30.

5 Tang A, Hallouch O, Chernyak V, Kamaya A, Sirlin CB. Epidemiology of hepatocellular carcinoma: target population for surveillance and diagnosis. Abdom Radiol. 2018;43(1):13–25.

6 van der Pol CB, McInnes MDF, Salameh JP, Levis B, Chernyak V, Sirlin CB, et al. CT/MRI and CEUS LI-RADS major features association with hepatocellular carcinoma: individual patient data meta-analysis. Radiology. 2022;302(2):326–35.

7 Choi JY, Lee JM, Sirlin CB. CT and MR imaging diagnosis and staging of hepatocellular carcinoma: part II. Extracellular agents, hepa-

tobiliary agents, and ancillary imaging features. Radiology. 2014;273(1):30–50.

8 Murakami T, Tsurusaki M. Hypervascular benign and malignant liver tumors that require differentiation from hepatocellular carcinoma: key points of imaging diagnosis. Liver Cancer. 2014;3(2):85–96.

9 Miyayama S, Yamashiro M, Okuda M, Yoshie Y, Nakashima Y, Ikeno H, et al. Detection of corona enhancement of hypervascular hepatocellular carcinoma by C-arm dual-phase cone-beam CT during hepatic arteriography. Cardiovasc Intervent Radiol. 2011;34(1):81–6.

10 Kitao A, Zen Y, Matsui O, Gabata T, Nakanuma Y. Hepatocarcinogenesis: multistep changes of drainage vessels at CT during arterial portography and hepatic arteriography: radiologic-pathologic correlation. Radiology. 2009; 252(2):605–14.

11 Kitao A, Matsui O, Yoneda N, Kita R, Kozaka K, Kobayashi S, et al. Differentiation between hepatocellular carcinoma showing hyperintensity on the hepatobiliary phase of gadoxetic acid-Enhanced MRI and focal nodular hyperplasia by CT and MRI. AJR Am J Roentgenol. 2018;211(2):347–57.

12 Patella F, Pesapane F, Fumarola EM, Emili I, Spairani R, Angileri SA, et al. CT-MRI LI-RADS v2017: a comprehensive guide for beginners. J Clin Transl Hepatol. 2018;286(2):222–36.

13 Willatt J, Ruma JA, Azar SF, Dasika NL, Syed F. Imaging of hepatocellular carcinoma and image guided therapies - how we do it. Cancer Imaging. 2017 4;17(1):9.

14 Wei Y, Ye Z, Yuan Y, Huang Z, Wei X, Zhang T, et al. A new diagnostic criterion with gadoxetic acid-enhanced MRI may improve the diagnostic performance for hepatocellular carcinoma. Liver Cancer. 2020;9(4):414–25.

15 Asayama Y, Yoshimitsu K, Nishihara Y, Irie H, Aishima S, Taketomi A. Arterial blood supply of hepatocellular carcinoma and histologic grading: radiologic-pathologic correlation. AJR Am J Roentgenol. 2008;190(1):W28–34.

16 Lee JH, Lee JM, Kim SJ, Baek JH, Yun SH, Kim KW, et al. Enhancement patterns of hepatocellular carcinomas on multiphasic multidetector row CT: comparison with pathological differentiation. Br J Radiol. 2012;85(1017):e573–83.

17 Van Beers BE, Pastor CM, Hussain HK. Primovist, eovist: what to expect? J Hepatol. 2012;57(2):421–9.

18 Torbenson MS, Ng IOL, Park YN, Roncalli M, Sakamoto M. Hepatocellular carcinoma. 5th ed. WHO Classification of Tumours Editorial BoardWHO classification of tumours: digestive system tumours. International Agency for Research on Cancer; 2019. p. 229–39.

19 Loy LM, Low HM, Choi JY, Rhee H, Wong CF, Tan CH. Variant hepatocellular carcinoma subtypes according to the 2019 WHO classification: an imaging-focused review. AJR Am J Roentgenol. 2022:1–12.

20 Kim JH, Joo I, Lee JM. Atypical appearance of hepatocellular carcinoma and its mimickers: how to solve challenging cases using gadoxetic acid-enhanced liver magnetic resonance imaging. Korean J Radiol. 2019;20(7):1019–41.

21 Liao SH, Su TH, Jeng YM, Liang PC, Chen DS, Chen CH, et al. Clinical manifestations and outcomes of patients with sarcomatoid hepatocellular carcinoma. Hepatology. 2019; 69(1):209–21.

22 Wang JP, Yao ZG, Sun YW, Liu XH, Sun FK, Lin CH, et al. Clinicopathological characteristics and surgical outcomes of sarcomatoid hepatocellular carcinoma. World J Gastroenterol. 2020 7;26(29):4327–42.

23 Beaufrère A, Calderaro J, Paradis V. Combined hepatocellular-cholangiocarcinoma: an update. J Hepatol. 2021;74(5):1212–24.

24 Gigante E, Ronot M, Bertin C, Ciolina M, Bouattour M, Dondero F, et al. Combining imaging and tumour biopsy improves the diagnosis of combined hepatocellular-cholangiocarcinoma. Liver Int. 2019;39(12):2386–96.

25 Namasivayam S, Martin DR, Saini S. Imaging of liver metastases: MRI. Cancer Imaging. 2007;7(1):2–9.

26 Li R, Cai P, Ma KS, Ding SY, Guo DY, Yan XC. Dynamic enhancement patterns of intrahepatic cholangiocarcinoma in cirrhosis on contrast-enhanced computed tomography: risk of misdiagnosis as hepatocellular carcinoma. Sci Rep. 2016;6(6):26772.

27 Rimola J, Forner A, Reig M, Vilana R, de Lope CR, Ayuso C. Cholangiocarcinoma in cirrhosis: absence of contrast washout in delayed phases by magnetic resonance imaging avoids misdiagnosis of hepatocellular carcinoma. Hepatology. 2009;50(3):791–8.

28 Bioulac-Sage P, Rebouissou S, Thomas C, Blanc JF, Saric J, Sa Cunha A, et al. Hepatocellular adenoma subtype classification using molecular markers and immunohistochemistry. Hepatology. 2007;46(3):740–8.

29 Kim TH, Woo S, Ebrahimzadeh S, Mclnnes MDF, Gerst SR, Do RK. Hepatic adenoma subtypes on hepatobiliary phase of gadoxetic acid-enhanced MRI: systematic review and meta-analysis. Am J Roentgenology. 2022;26:1–11.

30 Barbier L, Nault JC, Dujardin F, Scotto B, Besson M, de Muret A, et al. Natural history of liver adenomatosis: a long-term observational study. J Hepatol. 2019;71(6):1184–92.

31 Mounajjed T. Hepatocellular adenoma and focal nodular hyperplasia. Clin Liver Dis. 2021 May 1;17(4):244–8.

32 Grazioli L, Morana G, Kirchin MA, Schneider G. Accurate differentiation of focal nodular hyperplasia from hepatic adenoma at gadobenate dimeglumine-enhanced MR imaging: prospective study. Radiology. 2005;236(1):166–77.

33 Sasaki M, Yoneda N, Kitamura S, Sato Y, Nakanuma Y. A serum amyloid A-positive hepatocellular neoplasm arising in alcoholic cirrhosis: a previously unrecognized type of inflammatory hepatocellular tumor. Mod Pathol. 2012;25(12):1584–93.

34 Lee SJ, Kim SY, Kim KW, Kim JH, Kim HJ, Lee MG, et al. Hepatic angiomyolipoma versus hepatocellular carcinoma in the noncirrhotic liver on gadoxetic acid-enhanced MRI: a diagnostic challenge. AJR Am J Roentgenol. 2016;207(3):562–70.

35 Jeon TY, Kim SH, Lim HK, Lee WJ. Assessment of triple-phase CT findings for the differentiation of fat-deficient hepatic angiomyolipoma from hepatocellular carcinoma in non-cirrhotic liver. Eur J Radiol. 2010;73(3):601–6.

36 Choi HHI, Manning MA, Mehrotra AK, Wagner S, Jha RC. Primary hepatic neoplasms of vascular origin: key imaging features and differential diagnoses with radiology-pathology correlation. AJR Am J Roentgenol. 2017;209(6):W350–9.

37 Zhou Y, Hou P, Wang F, Li B, Gao J. Primary hepatic malignant vascular tumors: a follow-up study of imaging characteristics and clinicopathological features. Cancer Imaging. 2020;1420(1):59.

38 Alturkistany S, Jang HJ, Yu H, Lee KH, Kim TK. Fading hepatic hemangiomas on multiphasic CT. Abdom Imaging. 2012; 37(5):775–80.

39 Yoshida K, Kobayashi S, Matsui O, Gabata T, Sanada J, Koda W, et al. Hepatic pseudolymphoma: imaging-pathologic correlation with special reference to hemodynamic analysis. Abdom Imaging. 2013;38(6):1277–85.

40 Sonomura T, Anami S, Takeuchi T, Nakai M, Sahara S, Tanihata H, et al. Reactive lymphoid hyperplasia of the liver: perinodular enhancement on contrast-enhanced computed tomography and magnetic resonance imaging. World J Gastroenterol. 2015;21(21):6759–63.

41 Vilgrain V, Lagadec M, Ronot M. Pitfalls in liver imaging. Radiology. 2016;278(1):34–51.

42 LeCun Y, Bengio Y, Hinton G. Deep learning. Nature. 2015 28;521(7553):436–44.

43 Das A, Acharya UR, Panda SS, Sabut S. Deep learning based liver cancer detection using watershed transform and Gaussian mixture model techniques. Cogn Syst Res. 2019;54:165–75.

44 Stollmayer R, Budai BK, Tóth A, Kalina I, Hartmann E, Szoldán P, et al. Diagnosis of focal liver lesions with deep learning-based multi-channel analysis of hepatocyte-specific contrast-enhanced magnetic resonance imaging. World J Gastroenterol. 2021 21;27(35):5978–88.

45 Hamm CA, Wang CJ, Savic LJ, Ferrante M, Schobert I, Schlachter T, et al. Deep learning for liver tumor diagnosis part I: development of a convolutional neural network classifier for multi-phasic MRI. Eur Radiol. 2019;29(7):3338–47.

46 Yamashita R, Mittendorf A, Zhu Z, Fowler KJ, Santillan CS, Sirlin CB, et al. Deep convolutional neural network applied to the liver imaging reporting and data system (LI-RADS) version 2014 category classification: a pilot study. Abdom Radiol (Ny). 2020;45(1):24–35.

47 Laino ME, Viganò L, Ammirabile A, Lofino L, Generali E, Francone M, et al. The added value of artificial intelligence to LI-RADS categorization: a systematic review. Eur J Radiol. 2022;150:110251.

48 Nam D, Chapiro J, Paradis V, Seraphin TP, Kather JN. Artificial intelligence in liver diseases: improving diagnostics, prognostics and response prediction. JHEP Rep. 2022 2;4(4):100443.

49 Su TH, Wu CH, Kao JH. Artificial intelligence in precision medicine in hepatology. J Gastroenterol Hepatol. 2021;36(3):569–80.

50 Wu Y, White GM, Cornelius T, Gowdar I, Ansari MH, Supanich MP, et al. Deep learning LI-RADS grading system based on contrast enhanced multiphase MRI for differentiation between LR-3 and LR-4/LR-5 liver tumors. Ann Transl Med. 2020;8(11):701.